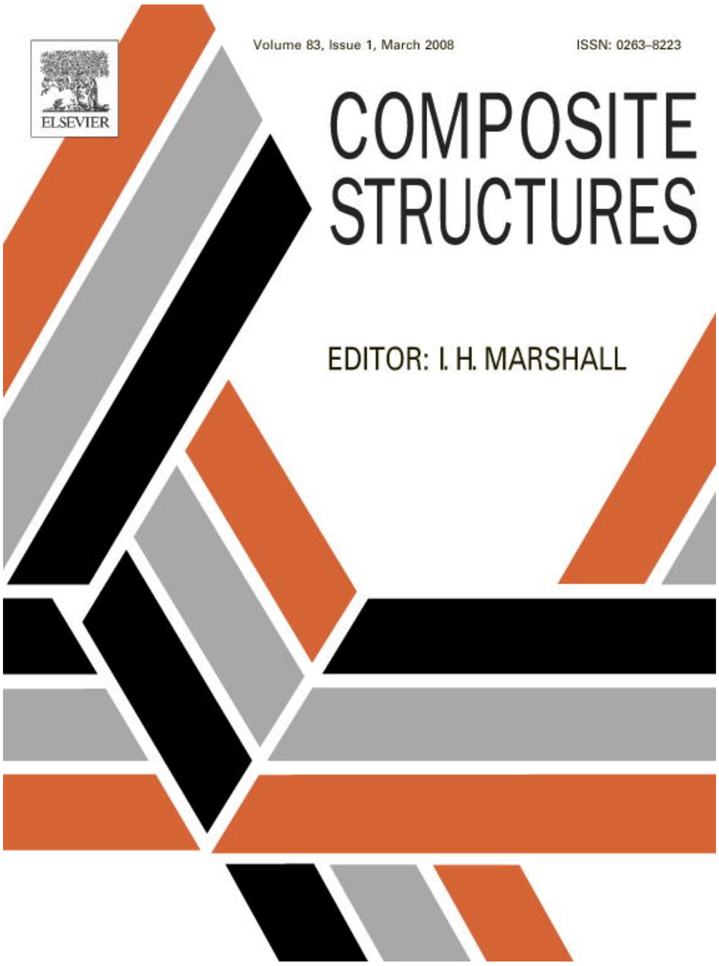
Volume 83, Issue 1, March 2008
ISSN: 0263-8223
ELSEVIER
COMPOSITE
STRUCTURES
EDITOR: I. H. MARSHALL

Available online at www.sciencedirect.com
ScienceDirect
ELSEVIER
Composite Structures 83 (2008) 83–92
COMPOSITE STRUCTURES
www.elsevier.com/locate/compstruct

Untruncated infinite series superposition method for accurate flexural analysis of isotropic/orthotropic rectangular plates with arbitrary edge conditions

K. Bhaskar *, A. Sivaram

Aerospace Engineering Department, Indian Institute of Technology, Madras, Chennai 600 036, India

Available online 14 April 2007

Abstract

A new elegant, powerful and accurate superposition method is presented for isotropic/specially orthotropic rectangular plates with arbitrary transverse load and arbitrary combination of free/simply-supported/clamped/guided/elastically supported edges. All the component solutions used here are infinite series equivalents of the complicated closed-form Levy-type solutions employed in the conventional superposition method; it is shown that these series equivalents are easily derived. The mathematical equations pertaining to the various component solutions required for the application of this new method to any plate problem are clearly presented. A number of validation studies are carried out to verify the accuracy of the method. The method can be directly extended to the analysis of more complicated plates made of multifunctional or functionally graded materials.

Keywords: Rectangular plates; Orthotropic plates; Analytical solution; Superposition method

1. Introduction

Plate structures are encountered in all fields of engineering and hence there is a rich history of the literature on the analysis of plates of various shapes using a variety of methods [1–3]. Of all the available solutions, those based on an exact analytical approach, wherein the governing equations and the boundary conditions are satisfied rigorously, are valuable; there is renewed interest in such classical solutions originally developed for simple metallic plates because the solution methodologies are often applicable with minor changes to modern state-of-the-art laminated plate structures made up of functionally graded materials or those with magneto-electro-thermo-elastic coupling effects [4,5, for example]. Further, it is well-known that such computationally efficient analytical solutions are invaluable in identifying the influences of various structural and material parameters, and in subsequent optimization exercises. In this context, the objective of this work is to put forth an elegant alternative to the conventional superposition method, with specific reference to the title problem as a first step; this is done below after the relevant literature survey.

While simple closed-form solutions are available for some problems like symmetrical bending of isotropic circular plates or bending of a uniformly loaded clamped elliptical plate, the analysis of rectangular plates requires the use of convergent series. The simplest solutions are those of Navier for a plate simply supported on all edges and Levy for one with two opposite edges simply supported [3]. A wider class of boundary conditions involving clamped edges can be handled analytically by the classical superposition method wherein the above Navier or Levy solutions are appropriately superposed with solutions accounting for harmonically distributed moments applied on different edges; the method should be termed exact since a convergent Fourier series representation is valid for the fixed edge moments, and the boundary conditions can be satisfied to any degree of accuracy by taking an appropri-

* Corresponding author. Tel.: +91 44 22574010; fax: +91 44 22574002. *E-mail address:* kbhas@ae.iitm.ac.in (K. Bhaskar).

0263-8223/$ - see front matter © 2007 Elsevier Ltd. All rights reserved.
doi:10.1016/j.compstruct.2007.04.001

ate number of terms in the series. This method has been amply illustrated for static flexure problems by Timoshenko and Krieger [1] and for vibration and stability problems by Gorman [6] who also extended it to plates with free edges.

It has been shown [7] that both Navier and Levy methods can be simply extended to *specially orthotropic* plates (i.e. with the axes of orthotropy parallel to the edges) and symmetric cross-ply laminates; however, while no additional complexity is encountered in the former, the final form of the Levy solution for the orthotropic plate depends on the roots of a characteristic equation and may involve products of polynomial and hyperbolic functions or trigonometric and hyperbolic functions instead of just hyperbolic functions.

It is also known [8] that Navier-type solutions are possible for two unsymmetric laminate configurations – an unsymmetric cross-ply plate with simply supported edges of the shear diaphragm type (called S2 type), and an antisymmetric angle-ply plate with simply supported edges which permit the in-plane tangential displacement freely but completely restrain the in-plane normal displacement (called S3 type). The corresponding counterparts with two simply supported opposite edges are amenable to Levy-type analysis, but this becomes rather cumbersome because of the need to solve three coupled ordinary differential equations which lead to a high-degree characteristic equation with various possible combinations of real and distinct or repeated or complex roots; a formal solution using the state-space technique is often employed, but this would still involve Jordan canonical transformations depending on the nature of the roots [9].

While the simple Levy type solutions for isotropic homogeneous plates are easy to superpose for obtaining solutions for plates with general boundary conditions, the more complicated ones for homogenous or laminated anisotropic plates present serious difficulties for use with the classical superposition method. These difficulties have been discussed quite elaborately by Gorman and Ding [10,11] with reference to free vibration analysis; in fact, it has also been pointed out that additional difficulties arise in numerical calculations because of hyperbolic functions with large arguments. These numerical difficulties arise even for isotropic homogeneous plates as had been pointed out earlier [12]. As an easy way out of all the difficulties, a Galerkin type approximate procedure was employed in Refs. [10,11] for generating the component solutions for laminated plates.

The afore-mentioned difficulties, which mainly arise because of coupled multiple differential equations of high order and the associated possibility of various root combinations, would get aggravated when one employs a refined shear deformation theory because any such theory is of higher order as compared to the classical Kirchhoff–Poisson thin plate theory. This additional complexity is readily seen in the studies on symmetric cross-ply plates [13] and antisymmetric angle-ply plates [14] using the Mindlin-type first-order theory.

Very recently, it has been shown [15] that an exact infinite Fourier series counterpart of the closed-form Levy type solution can be generated easily for an isotropic/specially orthotropic plate subjected to a harmonically varying moment applied along any edge, and such component solutions are easy to work with in a superposition approach for the analysis of plates with any combination of clamped and simply supported edges. It has also been proved that no loss of accuracy occurs if the infinite series are summed without truncation, such untruncated summation being possible using mathematical packages like *MATHEMATICA* or *MATLAB*. Thus, the difficulties mentioned earlier with respect to the Levy-type solutions are completely avoided without resorting to any approximations.

The objective of the present paper is to show that the above approach, hereafter referred to as untruncated infinite series superposition method (UISSM), is quite powerful in that it can be employed successfully for the most general and most complicated plate problems involving any combination of simply supported, clamped, free, guided and elastically supported edges (denoted herein by S, C, F, G and E, respectively); further, the transverse load can be quite arbitrary – for example, it can be a partial load on the plate, or a line load/moment or a concentrated load applied on a free edge. All the required building blocks are derived here for the case of symmetric cross-ply plates within the purview of classical lamination theory; it is shown that Stokes' transformation [16] is necessary for generating some derivatives of the deflection function. Complete equivalence with the conventional superposition method involving closed-form Levy type solutions is proved. Finally, tabulated results are presented for some cases for future comparisons.

2. The new method – UISSM

Rectangular plates ($0 \leqslant x \leqslant a$, $0 \leqslant y \leqslant b$) with an arbitrary combination of simply supported, clamped and free/guided edges are considered first; the plate may be isotropic homogeneous or a symmetric cross-ply laminate. The building blocks required in UISSM depend on the number of free/guided edges and hence are discussed separately under different categories as below. The extension of the method to account for elastic restraints is straightforward as explained later.

2.1. Category I: one free/guided edge (and also no free/guided edges)

The building blocks for this category are shown in Fig. 1; they are valid when the bottom edge ($y = b$) is taken to be free. As can be seen, they correspond to a plate either simply supported all around or with one guided edge (i.e. one that is free to translate but with the normal slope completely restrained), and subjected to transverse load or edge moment or edge shear force expressed without loss of generality in the following form:

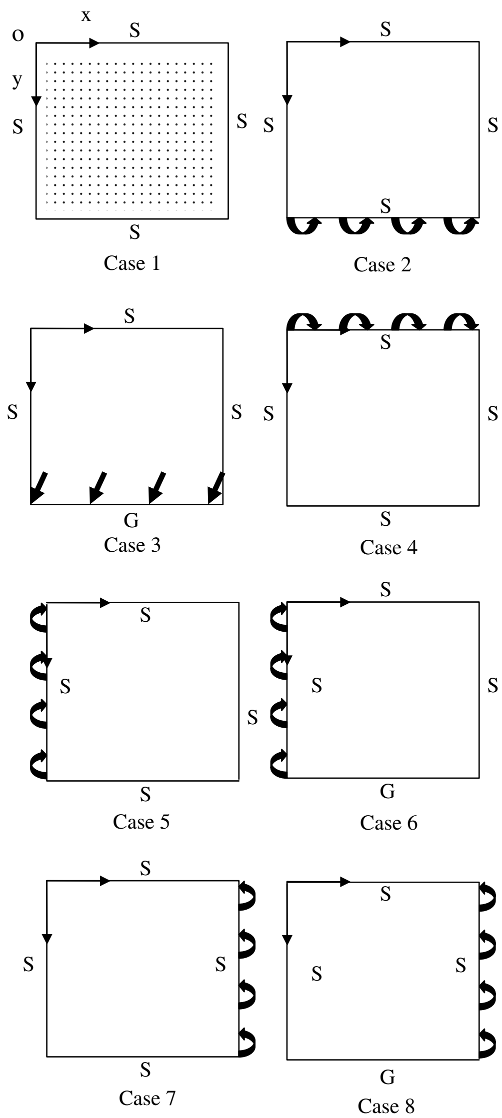

Fig. 1. Building blocks for Category I.

$$\begin{aligned}
&\text{Case 1}: q = \sum_m \sum_n q_{mn} \sin(m\pi x/a)\sin(n\pi y/b);\\
&\text{Case 2}: M_{\mathrm{b}} = \sum_m M_{\mathrm{b}m} \sin(m\pi x/a)\\
&\text{Case 3}: V_{\mathrm{b}} = \sum_m V_{\mathrm{b}m} \sin(m\pi x/a);\\
&\text{Case 4}: M_{\mathrm{t}} = \sum_m M_{\mathrm{t}m} \sin(m\pi x/a)\\
&\text{Case 5}: M_{\mathrm{l}} = \sum_n M_{\mathrm{l}n} \sin(n\pi y/b);\\
&\text{Case 6}: \overline{M}_{\mathrm{l}} = \sum_{n=1,3,\ldots} \overline{M}_{\mathrm{l}n} \sin(n\pi y/2b)\\
&\text{Case 7}: M_{\mathrm{r}} = \sum_n M_{\mathrm{r}n} \sin(n\pi y/b)\\
&\text{Case 8}: \overline{M}_{\mathrm{r}} = \sum_{n=1,3} \overline{M}_{\mathrm{r}n} \sin(n\pi y/2b)
\end{aligned} \tag{1}$$

The subscripts l, r, b and t (which will appear later) are used to denote the left, right, bottom and top edges, respectively. All the loads shown in Fig. 1 are positive as per the usual sign convention.

The conventional superposition method is based on the use of the closed-form Levy-type solutions. For example, for case 2 or 3 with just one harmonic (m) of the applied load, one starts with

$$w = W_m(y)\sin(m\pi x/a) \tag{2}$$

and obtains an ordinary differential equation in W_m by substituting in the governing equation of the plate

$$D_{11}w_{,xxxx} + 2(D_{12} + 2D_{66})w_{,xxyy} + D_{22}w_{,yyyy} = 0 \tag{3}$$

where D_{ij}'s are the orthotropic bending stiffness coefficients occurring in the moment-curvature relations

$$\begin{Bmatrix} M_x \\ M_y \\ M_{xy} \end{Bmatrix} = \begin{bmatrix} D_{11} & D_{12} & 0 \\ & D_{22} & 0 \\ \text{sym.} & & D_{66} \end{bmatrix} \begin{Bmatrix} -w_{,xx} \\ -w_{,yy} \\ -2w_{,xy} \end{Bmatrix} \tag{4}$$

If the plate is isotropic, we have $D_{11} = D_{22} = D$, $D_{12} = \nu D$, $D_{66} = D(1-\nu)/2$.

The ordinary differential equation is solved with appropriate conditions at the edges $y = 0$, b to yield W_m in closed-form; however, depending on the nature of the roots of the characteristic equation, which in turn depends on the material constants, the expression for W_m can be of three types [7] involving either hyperbolic functions alone, or products of hyperbolic functions with polynomial or trigonometric functions. Thus W_m cannot be written in a single generic form, and the expressions are inconveniently lengthy for superposition later.

The new method proposed here eliminates this difficulty by starting with a series representation for the unknown function, for example

$$\begin{aligned}
w &= \left(\sum_{n=1}^{\infty} W_{mn}\sin(n\pi y/b)\right)\sin(m\pi x/a) \text{ for case 2,}\\
&\times \left(\sum_{n=1,3,\ldots}^{\infty} W_{mn}\sin(n\pi y/2b)\right)\sin(m\pi x/a) \text{ for case 3}
\end{aligned} \tag{5}$$

Such a Fourier series representation is perfectly legitimate for the deflection function because of its continuous nature over the domain and because the zero or non-zero w conditions at $y = 0,b$ are satisfied by each term of the series.

The unknown coefficients W_{mn} cannot, however, be determined by using the governing equation (Eq. (3)) because the series of Eq. (5) cannot be differentiated term-wise for obtaining the fourth-order derivatives occurring in Eq. (3). For example, for case 2, $w_{,yy}$ as obtained from Eq. (5) turns out to be zero at $y = b$, while it is actually non-zero and related to the bending moment M_y applied at that edge; similarly, for case 3, $w_{,yyy}$ turns out to be zero at $y = b$, while it should be proportional to the applied edge force V_y. Hence, further derivatives cannot be obtained by simple term-by-term differentiation.

To determine W_{mn}, one must instead invoke the principle of virtual work given by

$$\begin{aligned}
&\int\int(-M_x\delta w_{,xx} - M_y\delta w_{,yy} - 2M_{xy}\delta w_{,xy})\,\mathrm{d}x\,\mathrm{d}y \\
&\quad = \int_{x=0}^{a} M_{\mathrm{b}m}\sin(m\pi x/a)(-\delta w_{,y})|_{y=b}\,\mathrm{d}x \text{ for case 2,} \\
&\int\int(-M_x\delta w_{,xx} - M_y\delta w_{,yy} - 2M_{xy}\delta w_{,xy})\,\mathrm{d}x\,\mathrm{d}y \\
&\quad = \int_{x=0}^{a} V_{\mathrm{b}m}\sin(m\pi x/a)(\delta w)|_{y=b}\,\mathrm{d}x \text{ for case 3}
\end{aligned} \tag{6}$$

Very clearly, all the derivatives occurring in Eq. (6) can be obtained by term-by-term differentiation of Eq. (5). Substitution of these expressions in Eq. (6) and use of the orthogonality relations of the trigonometric functions given by

$$\begin{aligned}
&\int_{s=0}^{l}\sin(\alpha\pi s/l)\sin(\beta\pi s/l)\,\mathrm{d}s \\
&\quad = \int_{s=0}^{l}\cos(\alpha\pi s/l)\cos(\beta\pi s/l)\,\mathrm{d}s = l/2 \text{ for } \alpha=\beta, \\
&\quad\quad 0 \text{ for } \alpha\neq\beta
\end{aligned} \tag{7}$$

yields W_{mn} as

$$\begin{aligned}
W_{mn} = &-n\pi a M_{\mathrm{b}m}\cos n\pi/2b\Gamma(a,b) \text{ for case 2,} \\
&V_{\mathrm{b}m}a\sin(n\pi/2)/\Gamma(a,2b) \text{ for case 3}
\end{aligned} \tag{8}$$

where the function Γ is given by

$$\begin{aligned}
\Gamma(\alpha,\beta) = \pi^4&\left[\beta^4 D_{11}m^4 + 2\alpha^2\beta^2(D_{12}+2D_{66})m^2n^2+\alpha^4 D_{22}n^4\right] \\
&/4\alpha^3\beta^3
\end{aligned} \tag{9}$$

It has to be pointed out that the closed-form $W_m(y)$ (Eq. (2)) of the conventional Levy-type approach and the alternative sine series in y with coefficients W_{mn} (Eq. (5)) employed in the present approach are analytically equivalent to each other. To prove this, the conventional Levy-type solution is explicitly derived below for load case 2; this is done for the special case of Huber orthotropy [1], for which

$$D_{12} + 2D_{66} = \sqrt{D_{11}D_{22}} \tag{10}$$

and the ordinary differential equation resulting from substitution of the assumed Levy-type solution as in Eq. (2) into the governing equation is

$$D_{11}\left(\frac{m\pi}{a}\right)^4 W_m - 2\sqrt{D_{11}D_{22}}\left(\frac{m\pi}{a}\right)^2 W''_m + D_{22}W^{iv}_m = 0 \tag{11}$$

The solution of this equation, with the boundary conditions corresponding to load case 2 (Fig. 1) with just one harmonic (m) of the applied edge moment, is given by

$$W_m = \frac{M_{\mathrm{b}m}a\lambda}{2m\pi D_{22}}\operatorname{cosech}\frac{m\pi b}{a\lambda}\left(b\coth\frac{m\pi b}{a\lambda}\sinh\frac{m\pi y}{a\lambda} - y\cosh\frac{m\pi y}{a\lambda}\right) \tag{12a}$$

where $\lambda^4 = D_{22}/D_{11}$.

Now, if one expands this function in a Fourier sine series (see Eq. (5)), the Fourier coefficients as obtained from the Euler formulae turn out to be

$$W_{mn} = -\frac{2M_{\mathrm{b}m}a^4b^2n\cos(n\pi)}{\pi^3\left(b^2m^2\sqrt{D_{11}} + a^2n^2\sqrt{D_{22}}\right)^2} \tag{12b}$$

which are the same as those of Eq. (8) when specialized for Huber orthotropy.

Thus, the present approach yields the infinite series counterparts of the closed-form Levy-type solutions and is hence equally accurate provided the infinite series are employed without truncation for further calculations. The main advantage of the present approach is that the infinite series solutions given by Eqs. (5) and (8) remain unaffected by the nature of the roots of the auxiliary equation unlike the Levy-type counterparts, and their concise form makes them ideal component solutions for use with a superposition approach.

The infinite series solutions corresponding to the other building blocks of Fig. 1 are obtained in the same manner as above, and all the solutions are given in Appendix A; that for case 1 involving a distributed transverse load turns out to be identically the same as the Navier-type solution. It should be pointed out that all these building blocks are required only for a CCCF plate (given in clockwise order starting from the left edge), while for other boundary condition combinations (SSSF, SSCF, etc.), some of them would suffice. For example, for an SSSF plate, cases 1–3 are sufficient.

The unknowns M_{bm} and V_{bm} are found out by imposing the actual boundary conditions on the superposed net solution. The relevant boundary conditions for the free edge are:

$$M_y = 0, V_y = Q_y + M_{xy,x} = M_{y,y} + 2M_{xy,x} = 0 \text{ at } y = b \tag{13}$$

where the contributions from each case are calculated using the corresponding infinite series solution for w along with the moment-curvature relations (Eq. (4)), while the edge loads M_{bot} and V_{bot} are taken directly for cases 2 and 3, respectively. As has been pointed out earlier, term-by-term differentiation of the infinite series for w is not valid for case 2 to obtain $w_{,yyy}$ which is required for calculating V_y; this difficulty is overcome by using Stokes' transformation as explained in Appendix A.

The final form of the boundary conditions of Eq. (13), for the example case of an SSSF plate with uniformly distributed load q_o, would be

$$\begin{aligned}
&\sum_{m=1,3,\ldots} M_{\mathrm{b}m}\sin(m\pi x/a) \\
&\quad + \sum_{m=1,3,\ldots} V_{\mathrm{b}m}\sin(m\pi x/a)\sum_{n=1,3,\ldots}^{\infty}(\ldots)\sin(n\pi/2) = 0 \\
&\text{i.e. } M_{\mathrm{b}m} + V_{\mathrm{b}m}\sum_{n=1,3,\ldots}^{\infty}(\ldots)\sin(n\pi/2) = 0 \\
&\quad\quad \text{for } m = 1,3,\ldots,m_{\max}
\end{aligned} \tag{14a}$$

and similarly,

$$q_o \sum_{n=1,3,\ldots}^{\infty} (\ldots)\cos n\pi + M_{bm}\left[(\ldots) + \sum_{n=1,2,\ldots}^{\infty}(\ldots)\cos n\pi\right] + V_{bm} = 0 \text{ for } m = 1,3,\ldots m_{\max} \tag{14b}$$

where only odd values of m occur in view of the symmetry of deformation about $x = a/2$. The bracketed quantities in these equations depend on m and n and the material constants. It is very important to note that the infinite summations occurring in these equations have to be summed without truncation so that the accuracy of the component solutions is not lost. Such untruncated summation, with the upper limit taken as infinity, is possible using *MATHEMATICA* or *MATLAB*; the basic idea is to express the infinite sum in terms of appropriate special functions like the gamma function. The accuracy of such a summation has already been well authenticated by comparison with closed-form Levy-type counterparts with reference to clamped/simply supported plates [15]. A similar comparison is presented for plates with free edges later on in this paper to validate not just the accuracy of the untruncated summation but also the adequacy of the superposed building blocks.

If there is a line load/moment or a concentrated load applied along the free edge, it is simply expanded in a sine series and taken on the right-hand side of Eq. (14). If any of the simply supported edges is clamped, additional building blocks from Fig. 1 come into picture. For example, if the top edge is clamped, case 4 is required, with the unknown moment coefficients M_{tm} determined by imposing the zero slope condition on this edge. If the left edge is clamped, both cases 5 and 6 are required; this is because the contribution to $w_{,x}$ at this edge from cases 1 and 2 has a sinusoidal variation of the form $\sin(n\pi y/b)$ which can be neutralized by a corresponding variation of the bending moment (case 5) while the contribution from case 3 is of the form $\sin(n\pi y/2b)$ which requires a moment as in case 6.

If the bottom edge is guided instead of being free, the building blocks of Fig. 1 are still applicable; only the zero M_y condition of Eq. (13) is replaced by the zero $w_{,y}$ condition. Alternatively, it is possible to solve this problem easily by mirror-imaging it about the guided edge.

If the plate has no free/guided edges at all, cases 1, 2, 4, 5 and 7 are the only ones required for any combination of simply supported/clamped edges as discussed earlier [15].

2.2. Category II: two opposite free/guided edges (at $y = 0, b$)

The building blocks required for this category, in addition to those shown in Fig. 1, are as in Fig. 2; the loads are taken to be

$$\begin{aligned} &\text{Case 9}: V_t = \sum_m V_{tm}\sin(m\pi x/a);\\ &\text{Case 10}: \widehat{M}_l = \sum_{n=1,3} \widehat{M}_{ln}\cos(n\pi y/2b);\\ &\text{Case 11}: \widehat{M}_r = \sum_{n=1,3} \widehat{M}_{rn}\cos(n\pi y/2b) \end{aligned} \tag{15}$$

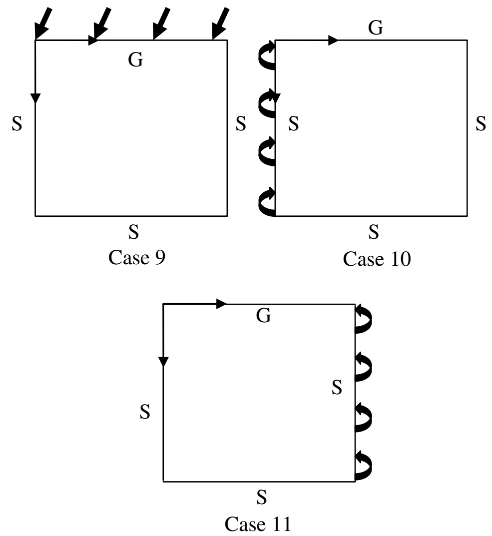

Fig. 2. Additional building blocks required for Category II with respect to Category I.

Case 9 is the counterpart of case 3 and necessary along with case 4 to impose the free/guided edge condition at the top. Further, cases 10 and 11, which are counterparts of cases 6 and 8, respectively, are necessary to neutralise the contributions of the form $\cos(n\pi y/2b)$ from case 9 to the slope $w_{,x}$ at the left and right edges, if they are clamped. The solutions for the new building blocks can be simply written down directly by analogy with those of Fig. 1, and are given in Appendix A. The enforcement of the boundary conditions to determine the unknown moment and shear coefficients is always similar to that illustrated in Eq. (14). For cases involving edge moments, the shear force contributions are always calculated using Stokes' transformation for the appropriate derivatives.

2.3. Category III: two adjacent free/guided edges (at $x = a$ and $y = b$)

The additional building blocks required for this category, besides those of Fig. 1, are shown in Fig. 3, with the loads given by

$$\begin{aligned} &\text{Case 12}: V_r = \sum_n V_{rn}\sin(n\pi y/b);\\ &\text{Case 13}: \overline{V}_b = \sum_{m=1,3} \overline{V}_{bm}\sin(m\pi x/2a)\\ &\text{Case 14}: \overline{V}_r = \sum_{n=1,3} \overline{V}_{rn}\sin(n\pi y/2b);\\ &\text{Case 15}: \overline{M}_b = \sum_{m=1,3} \overline{M}_{bm}\sin(m\pi x/2a)\\ &\text{Case 16}: \overline{M}_t = \sum_{m=1,3} \overline{M}_{tm}\sin(m\pi x/2a) \end{aligned} \tag{16}$$

Case 12 is required along with case 7 for imposing the free/guided edge conditions at the right edge. In addition, one

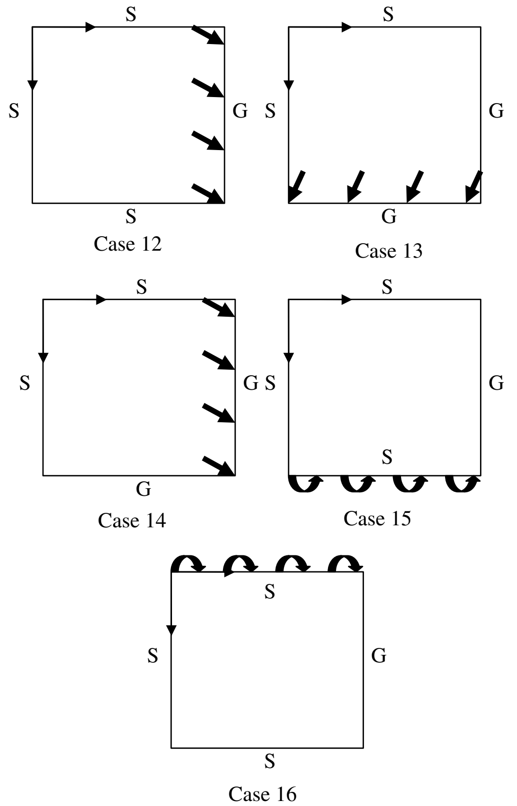

Fig. 3. Additional building blocks required for Category III with respect to Category I.

can see that contributions to the shear force along $y = b$ occur in the form $\sin(m\pi x/a)$ as well as $\sin(m\pi x/2a)$ (from case 12) and hence case 13 is required besides case 3 for their neutralization; similarly, case 14 is required besides case 12. In turn, due to cases 13 and 14, bending moments of the forms $\sin(m\pi x/2a)$ and $\sin(n\pi y/2b)$ are generated along $y = b$ and $x = a$, respectively, and have to be neutralized by cases 15 and 8. Finally, to take care of clamped edge conditions at the left or top edge, case 16 is required in addition to cases 4, 5 and 6.

As with Category I, the method of images can also be used advantageously for cases involving guided edges here.

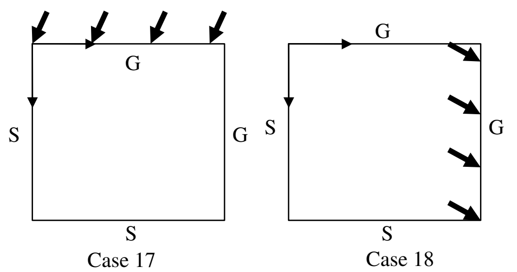

Fig. 4. Additional building blocks required for Category IV with respect to Categories II and III.

2.4. Category IV: three free/guided edges (except at $x = 0$)

It is easy to see that all the building blocks discussed so far (Cases 1–16) are required for this category, and also those of Fig. 4 with the following loads:

$$\begin{aligned} &\text{Case 17}: \overline{V}_t = \sum_{m=1,3} \overline{V}_{tm} \sin(m\pi x/2a); \\ &\text{Case 18}: \widehat{V}_r = \sum_{n=1,3} \widehat{V}_{rn} \cos(n\pi y/2b). \end{aligned} \tag{17}$$

2.5. Elastic supports

The elastic restraint at an edge may be against rotation or translation or both. Rotationally restrained edges are treated similar to clamped edges in UISSM and require the same building blocks; only the zero slope condition is replaced by a relation between the slope and the net bending moment. For example, for an SSSE plate with rotational restraint at the bottom edge, cases 1 and 2 (Fig. 1) are sufficient as for an SSSC plate; both the net slope $w_{,y}$ and the net bending moment M_y at the bottom edge vary as $\sum(\ldots)\sin(m\pi x/a)$ and hence the relation between them yields the unknowns M_{bm}.

Cases with elastic supports that restrain translation alone, or rotation as well as translation, require the same building blocks as those with free edges. For instance, such an SSSE plate would require cases 1–3 (Fig. 1) with the unknowns M_{bm} and V_{bm} obtained from the two boundary conditions at the elastic support. More complicated cases can be handled in a similar fashion and present no new difficulties as compared to cases involving free edges.

2.6. General observations about the method

Of all the problems discussed so far, that of a cantilevered plate (Category IV) is the most complicated in terms of the number of unknowns to be determined which turn out to be 17 sets of moment or shear force coefficients. However, even this problem is easily handled here in the sense that the unknowns are obtained from a corresponding set of simple algebraic equations obtained without tedious manipulations; the final solution so obtained is a simple combination of analytically exact component solutions which enable one to satisfy the boundary conditions to any desired degree of accuracy.

It should be mentioned that the number of building blocks required here is more than that in the conventional superposition method (see [17] for the cantilevered plate) because they have to be so chosen that simple double Fourier series solutions are applicable for them; however, this disadvantage is more than compensated by the simpler series solutions employed here as compared to the closed-form Levy type expressions which need to be derived separately for different root combinations and which often lead to computational difficulties because of hyperbolic functions with large arguments, as pointed out earlier. The benefits of the present approach would be much more significant if complicating effects such as bending-stretching coupling and shear deformation have to be accounted for, as has already been illustrated with reference to plates with simply supported/clamped edges [18–21].

3. Results and discussion

The main purpose of the present work is to present a more convenient alternative to the conventional superposition approach, and from this viewpoint it is of utmost importance that the new method be validated for its accuracy; for this purpose, three standard solutions available in the literature have been chosen. In addition to these validation studies, convergent results are tabulated for the sake of future comparisons for both isotropic and orthotropic plates with some chosen combinations of free, simply supported and clamped edges. The orthotropic properties considered correspond to a (0°) unidirectionally reinforced fiber composite with the following elastic constants:

$$E_L/E_T = 25, \quad G_{LT}/E_T = 0.5, \quad \nu_{LT} = 0.25$$

where L and T refer to the directions parallel and transverse, respectively, to the fibers. All calculations have been carried out using *MATHEMATICA*; For the sake of convenience, all the sine series for different moment and shear force coefficients are truncated such that the number of terms in each series is the same; the actual number of terms required is found to be in the range of 5–10 for convergence of the deflections and 15–30 for convergence of the moments. No numerical difficulties (due to overflow or underflow or ill-conditioned equations) are encountered even when a large number of terms are considered.

The first validation study is with respect to Hutchinson's solution [12] for uniformly loaded SSSF/SFSF/SCSF plates. This is a superior solution as compared to the conventional Levy-type solution found in text-books [1] because it eliminates numerical difficulties arising out of hyperbolic functions with large arguments by replacing them with modified hyperbolic functions, and yields results correct up to a larger number of significant digits. Comparison of these results with those of the present UISSM is shown in Table 1 to prove that they agree exactly up to five significant digits.

The second validation study is with respect to the solution of Thornton and Conway [22] for an SFSF plate with a concentrated point load on a free edge. Once again, this is an improved solution as compared to the conventional Levy-type solution because it eliminates slow convergence difficulties by means of splitting up of the final solution into a closed-form singular part and a fast convergent series part. The efficacy of the present methodology for this problem is demonstrated in Table 2, wherein results based on the solution of Thornton and Conway are those specifically generated for the present comparison study because their paper contains all results only in graphical form.

The third study is for plates with elastic supports; the problem is that of a SESE plate with the elastic supports corresponding to beams of flexural rigidity EI; they resist bending in the vertical planes only and do not resist tor-

Table 1
Validation of UISSM for uniformly loaded isotropic square plates ($\nu = 0.3$)

Plate	At $(a/2, b)$		At $(a/2, b/2)$	
	Dw/q_oa^4	M_x/q_oa^2	M_x/q_oa^2	M_y/q_oa^2
SSSF				
UISSM	0.012852	0.11170	0.079853	0.038981
Ref. [12]	0.012852	0.11170	0.079853	0.038981
SFSF				
UISSM	0.015011	0.13109	0.12255	0.027078
Ref. [12]	0.015011	0.13109	0.12255	0.027078
SCSF				
UISSM	0.011236	0.097185		−0.11841[a]
Ref. [12]	0.011236	0.097185		−0.11841

[a] At $(a/2, 0)$.

Table 2
Validation of UISSM for an isotropic SFSF square plate with a point load P at the center of a free edge ($\nu = 0.3$)

Method	Eh^3w/Pa^2 at loaded point	M_x/P at center	M_y/P at center
UISSM	0.64879	0.1640	−0.04685
Ref. [22]	0.64879	0.1640	−0.04685

Table 3
Validation of UISSM for a uniformly loaded isotropic SESE square plate with elastic beams at the E edges ($\nu = 0.3$)

EI/aD	Method	Dw/q_oa^4 at center	M_x/q_oa^2 at center	M_y/q_oa^2 at center
1	UISSM	0.00624	0.0659	0.0428
	Levy-type	0.00624	0.0659	0.0428
10	UISSM	0.00434	0.0502	0.0472
	Levy-type	0.00434	0.0502	0.0472
100	UISSM	0.00409	0.0481	0.0478
	Levy-type	0.00409	0.0481	0.0478

Table 4
Converged results for uniformly loaded isotropic square plates ($\nu = 0.3$)

Plate	At the center of free edge		M^a/q_oa^2 at center of clamped edge
	Eh^3w/q_oa^4	M^a/q_oa^2	
SSCF	0.06328 (0.06336[b])	0.0637 (0.0639)	−0.101 (−0.103)
SCCF	0.06020 (0.06027)	0.0604 (0.0604)	Top −0.0769 (−0.0771) Right −0.0835 (−0.0837)
CSCF	0.03246 (0.03250)	0.0440 (0.0442)	−0.0757 (−0.0758)
CCCF	0.03218 (0.03223)	0.0433 (0.0435)	Top −0.0561 (−0.0563) Right −0.0655 (−0.0657)
SFCF	0.06417 (0.06425)	0.0648 (0.0650)	−0.120 (−0.122)
CFCF	0.03173 (0.03177)	0.0433 (0.0434)	−0.0812 (−0.0815)
SSFF	1.126 (1.126)	0.117 (0.118)	
SCFF	Bottom 0.4823 (0.4828) Right 0.3253 (0.3259)	Bottom 0.0721 (0.0723) Right −0.0136 (−0.0137)	−0.250 (−0.252)
CCFF	0.2174 (0.2178)	0.00966 (0.00968)	−0.128 (−0.130)
CFFF	Bottom 0.4722 (0.4728) Right 1.408 (1.409)	Bottom −0.126 (−0.129) Right 0.0133 (0.0150)	−0.528 (−0.531)

[a] The non-zero tangential moment at a free edge; the normal (clamping) moment at a clamped edge.
[b] Finite element results using ANSYS are given in parentheses.

Table 5
Converged results for uniformly loaded orthotropic square plates

Plate	At the center of free edge		M^a/q_oa^2 at center of clamped edge
	$100E_Th^3w/q_oa^4$	M^a/q_oa^2	
SSSF	0.6466 (0.6467[b])	0.129 (0.129)	
SSCF	0.2556 (0.2561)	0.0641 (0.0642)	−0.127 (−0.127)
SCSF	0.6519 (0.6520)	0.130 (0.130)	−0.0249 (−0.0250)
SCCF	0.2557 (0.2560)	0.0641 (0.0642)	Top −0.0155 (−0.0156) Right −0.126 (−0.127)
CSCF	0.1274 (0.1277)	0.0428 (0.0429)	−0.0845 (−0.0846)
CCCF	0.1273 (0.1276)	0.0428 (0.0429)	Top −0.0109 (−0.0112) Right −0.0850 (−0.0852)
SFSF	0.6471 (0.6472)	0.129 (0.129)	
SFCF	0.2563 (0.2568)	0.0643 (0.0644)	−0.122 (−0.125)
CFCF	0.1275 (0.1278)	0.0428 (0.0429)	−0.0831 (−0.0833)
SSFF	Bottom 76.62 (76.68) Right 89.83 (89.88)	Bottom 0.300 (0.301) Right 0.112 (0.113)	
SCFF	Bottom 36.33 (36.40) Right 31.73 (31.78)	Bottom 0.211 (0.213) Right 0.00581 (0.00583)	−0.194 (−0.196)
CCFF	Bottom 2.288 (2.293) Right 4.214 (4.219)	Bottom −0.128 (−0.129) Right 0.0144 (0.0146)	Left −0.378 (−0.380) Top −0.0334 (−0.0335)
CFFF	Bottom 2.087 (2.092) Right 6.000 (6.005)	Bottom −0.125 (−0.127) Right 0.000337 (0.000339)	−0.499 (−0.502)

[a,b] As in Table 4.

sion. Results based on the conventional Levy-type solution [1] are shown to agree exactly with those of UISSM in Table 3. (It should be pointed out that the some of the results tabulated in the book of Timoshenko and Krieger [1] for this problem are erroneous; converged results obtained using the equations given therein have been used here.) The exact agreement observed in all the three validation studies confirms that the present methodology is accurate.

Finally, for the sake of future comparisons, converged results based on UISSM are tabulated in Tables 4–6 for a number of cases; plates without free edges are not included here because they have already been dealt with earlier [15]. Just for the sake of comparison, converged results based on finite element analysis with eight-noded plate elements and obtained using the commercial package *ANSYS* have also been included in these tables.

Table 6
Converged results for an SSSF square plate with a loaded free edge

Plate	Load at the free edge		
	Load p per unit length	Moment m_o per unit length	Concentrated load P at mid-point
Isotropic			
Deflection[a]	0.3806 (0.3819[b])	0.7742 (0.7756)	0.6361 (0.6373)
Moment[a]	0.290 (0.290)	0.217 (0.218)	
Orthotropic			
Deflection	0.04921 (0.05010)	0.2250 (0.2264)	0.08219 (0.08350)
Moment	0.937 (0.937)	3.52 (3.53)	

[a] Values at $(a/2, a)$; deflection normalized with respect to (pa^3/Eh^3) or (m_oa^2/Eh^3) or (Pa^2/Eh^3), or (pa^3/E_Th^3), etc.; moment normalized with respect to m_o or (pa).
[b] Finite element results using ANSYS.

4. Conclusion

A simpler and equally accurate alternative to the conventional superposition method has been presented here for the analysis of isotropic/symmetric cross-ply plates with arbitrary loads and edge conditions. The method enables one to attempt analytical solutions for problems which have hitherto been considered too complicated for rigorous study and hence analyzed using approximate and numerical approaches like the finite element method. It is also valuable in the light of the fact that results for deflections and moments cannot be tabulated in handbooks for orthotropic plates as for isotropic plates because they depend on the various orthotropic elastic constants.

As would be clear to anyone familiar with analysis of plates/shells, the present method can be directly extended for stability and vibration analysis of plates, studies involving various complicating effects such as unsymmetry of lamination, shear deformation and rotary inertia, hygrothermal loads, elastic foundations, magneto-electro-elastic coupling effects and continuous through-the-thickness inhomogeneity characteristic of functionally graded materials, as well as the corresponding cylindrical and shallow shell problems. Some such extensions will be reported in future.

Appendix A

The deflection w is obtained in the following form:

$$\begin{aligned} w &= \sum_m \sum_n W_{mn} \sin(m\pi x/a)\sin(n\pi y/b) \text{ for cases } 1,2,4,5,7 \\ w &= \sum_{m=1,3,\ldots} \sum_n W_{mn} \sin(m\pi x/2a)\sin(n\pi y/b) \text{ for cases } 12,15,16 \\ w &= \sum_m \sum_{n=1,3,\ldots} W_{mn} \sin(m\pi x/a)\sin(n\pi y/2b) \text{ for cases } 3,6,8 \\ w &= \sum_{m=1,3,\ldots} \sum_{n=1,3,\ldots} W_{mn} \sin(m\pi x/2a)\sin(n\pi y/2b) \text{ for cases } 13,14 \\ w &= \sum_m \sum_{n=1,3,\ldots} W_{mn} \sin(m\pi x/a)\cos(n\pi y/2b) \text{ for cases } 9,10,11 \\ w &= \sum_{m=1,3\ldots} \sum_{n=1,3,\ldots} W_{mn} \sin(m\pi x/2a)\cos(n\pi y/2b) \text{ for cases } 17,18 \end{aligned} \tag{A1}$$

where W_{mn} is given by

$$\begin{aligned} W_{mn} = {} & \frac{abq_{mn}}{4\Gamma(a,b)}(\text{case }1), \quad \text{or } \frac{-n\pi aM_{bm}\cos n\pi}{2b\Gamma(a,b)}(\text{case }2), \quad \text{or} \\ & \frac{V_{bm}a\sin(n\pi/2)}{\Gamma(a,2b)}(\text{case }3), \quad \text{or } \frac{n\pi aM_{tm}}{2b\Gamma(a,b)}(\text{case }4), \quad \text{or} \\ & \frac{m\pi bM_{ln}}{2a\Gamma(a,b)}(\text{case }5), \text{or } \frac{-m\pi bM_{rn}\cos m\pi}{2a\Gamma(a,b)}(\text{case }7), \quad \text{or} \\ & \frac{V_{tm}a}{\Gamma(a,2b)}(\text{case }9), \quad \text{or } \frac{m\pi b\hat{M}_{ln}}{a\Gamma(a,2b)}(\text{case }10), \quad \text{or} \\ & \frac{-m\pi b\hat{M}_{rn}\cos m\pi}{a\Gamma(a,2b)}(\text{case }11), \quad \text{or } \frac{V_{rn}b\sin(m\pi/2)}{\Gamma(2a,b)}(\text{case }12), \quad \text{or} \\ & \frac{2\hat{V}_{rn}b\sin(m\pi/2)}{\Gamma(2a,2b)}(\text{case }18) \end{aligned} \tag{A2}$$

For cases 15, 13, 16, 17, W_{mn} is obtained from cases 2, 3,4, 9, respectively, by changing a to $2a$ and the edge load coefficient to $\overline{M}_b$, $\overline{V}_b, \ldots$ as appropriate; similarly, that for cases 6, 8,14 is obtained from cases 5, 7, 12, respectively, by changing b to $2b$ and the edge load coefficient as appropriate.

All the required derivatives of w are obtained by termwise differentiation of the double Fourier series. However, for the load cases involving edge moments, the third derivatives with respect to x or y, as the case may be, cannot be obtained thus. This is because the corresponding second derivative violates the non-zero moment condition at the loaded edge. For example, for case 2 with just one harmonic (m) of the applied moment, one has

$$w_{,yy} = -\sum_n (n\pi/b)^2 W_{mn} \sin(n\pi y/b)\sin(m\pi x/a) \tag{A3}$$

which is applicable everywhere except at $y = b$, where it is zero while the correct value is given by

$$\begin{aligned} & M_y = -D_{12}w_{,xx} - D_{22}w_{,yy} \\ & \text{i.e. } w_{,yy} = -(M_{bm}/D_{22})\sin(m\pi x/a) \text{ since } w_{,xx} = 0 \end{aligned} \tag{A4}$$

Because of this violation of the end condition, further derivatives have to be obtained using Stokes' transformation. The basic idea is to assume

$$w_{,yyy} = \left(A_{m0} + \sum_{n=1,2,\ldots} A_{mn}\cos(n\pi y/b)\right)\sin(m\pi x/a) \tag{A5}$$

Integration of both sides of the above equation with respect to y between the limits 0 and b yields

$$w_{,yy}\big|_0^b = A_{m0}b\sin(m\pi x/a), \text{ and hence } A_{m0} = -M_{bm}/bD_{22} \tag{A6}$$

Similarly, multiplying both sides of Eq. (A5) by $\cos(n\pi y/b)$ and integrating with respect to y as before, one gets

$$w_{,yy}\cos(n\pi y/b)|_0^b + \int_0^b w_{,yy}(n\pi/b)\sin(n\pi y/b)\,dy = A_{mn}(b/2)\sin(m\pi x/a) \tag{A7}$$

Use of Eq. (A3) to evaluate the integral in the above equation finally yields

$$A_{mn} = -(2M_{bm}\cos n\pi)/bD_{22} - (n\pi/b)^3 W_{mn} \tag{A8}$$

and hence,

$$w_{,yyy} = \sum_m \left[-M_{bm}/bD_{22} - \sum_{n=1,2}\{2M_{bm}\cos n\pi/bD_{22} + (n\pi/b)^3 W_{mn}\}\cos(n\pi y/b) \right]\sin(m\pi x/a) \tag{A9}$$

for case 2 with the general moment load M_b.

The other derivatives obtained using this approach are as given below:

$$\begin{aligned}
\text{Case 4}: w_{,yyy} &= \sum_m \left[M_{tm}/bD_{22} + \sum_{n=1,2}\{2M_{tm}/bD_{22} - (n\pi/b)^3 W_{mn}\}\cos(n\pi y/b) \right]\sin(m\pi x/a) \\
\text{Case 5}: w_{,xxx} &= \sum_n \left[M_{ln}/aD_{11} + \sum_{m=1,2}\{2M_{ln}/aD_{11} - (m\pi/a)^3 W_{mn}\}\cos(m\pi x/a) \right]\sin(n\pi y/b) \\
\text{Case 7}: w_{,xxx} &= \sum_n \left[-\frac{M_{rn}}{aD_{11}} - \sum_{m=1,2}\left\{\frac{2M_{rn}\cos m\pi}{aD_{11}} + \left(\frac{m\pi}{a}\right)^3 W_{mn}\right\}\cos\frac{m\pi x}{a} \right]\sin\frac{n\pi y}{b} \\
\text{Case 10}: w_{,xxx} &= \sum_n \left[\frac{\hat{M}_{ln}}{aD_{11}} + \sum_{m=1,2}\left\{\frac{2\overline{M}_{ln}}{aD_{11}} - \left(\frac{m\pi}{a}\right)^3 W_{mn}\right\}\cos\frac{m\pi x}{a} \right]\cos\frac{n\pi y}{2b} \\
\text{Case 11}: w_{,xxx} &= \sum_n \left[-\frac{\widehat{M}_{rn}}{aD_{11}} - \sum_{m=1,2}\left\{\frac{2\widehat{M}_{rn}\cos m\pi}{aD_{11}} + \left(\frac{m\pi}{a}\right)^3 W_{mn}\right\}\cos\frac{m\pi x}{a} \right]\cos\frac{n\pi y}{2b}
\end{aligned} \tag{A10}$$

For cases 6 and 8, $w_{,xxx}$ is obtained from that of cases 5 and 7, respectively, by changing b to $2b$, and the moment coefficient as appropriate; similarly, for cases 15 and 16, $w_{,yyy}$ is obtained from that of cases 2 and 4, respectively, by changing a to $2a$, and the moment coefficient as appropriate.

References

[1] Timoshenko SP, Krieger SW. Theory of plates and shells. Tokyo: McGraw-Hill; 1959.
[2] Varadan TK, Bhaskar K. Analysis of plates. New Delhi: Narosa Publishing House; 1999.
[3] Szilard R. Theories and applications of plate analysis. New Jersey: Wiley; 2004.
[4] Abrate S. Free vibration, buckling, and static deflections of functionally graded plates. Compos Sci Technol 2006;66(14):2383–94.
[5] Kapuria S, Dube GP, Dumir PC, Sengupta S. Levy-type piezothermoelastic solution for hybrid plate by using first-order shear deformation theory. Composite B 1997;28(5–6):535–46.
[6] Gorman DJ. Vibration analysis of plates by the superposition method. Singapore: World Scientific; 1999.
[7] Lekhnitskii SG. Anisotropic plates. New York: Gordon & Breach; 1968.
[8] Whitney JM. Structural analysis of laminated anisotropic plates. Lancaster: Technomic; 1987.
[9] Franklin JN. Matrix theory. Englewood Cliffs (NJ): Prentice-Hall; 1968.
[10] Gorman DJ, Ding W. Accurate free vibration analysis of laminated symmetric cross-ply rectangular plates by the superposition-Galerkin method. Compos Struct 1995;31(2):129–36.
[11] Gorman DJ, Ding W. The superposition-Galerkin method for free vibration analysis of rectangular plates. J Sound Vib 1996;194(2):187–98.
[12] Hutchinson JR. On the bending of rectangular plates with two opposite edges simply supported. ASME J Appl Mech 1992;59(3):679–81.
[13] Yu SD, Cleghorn WI, Fenton RG. Free vibration and buckling of symmetric cross-ply rectangular laminates. AIAA J 1994;32(11):2300–8.
[14] Li N, Mirza S. Vibration of antisymmetric angle-ply laminated plates including transverse shear deformation. Mech Compos Mater Struct 1995;2(2):163–75.
[15] Bhaskar K, Kaushik B. Simple and exact series solutions for flexure of orthotropic rectangular plates with any combination of clamped and simply supported edges. Compos Struct 2004;63(1):63–8.
[16] Bromwich TJ. An introduction to the theory of infinite series. London: Macmillan; 1926.
[17] Gorman DJ. Accurate free vibration analysis of the orthotropic cantilever plate. J Sound Vib 1995;181(4):605–18.
[18] Bhaskar K, Kaushik B. Analysis of clamped unsymmetric cross-ply rectangular plates by superposition of simple exact double Fourier series solutions. Compos Struct 2005;68(3):303–7.
[19] Bhaskar K. An elegant and rigorous analytical solution for antisymmetric angle-ply rectangular plates with any combination of simply supported and clamped edges. J Reinforce Plast Compos 2006;25(16):1679–89.
[20] Umasree P, Bhaskar K. Accurate flexural analysis of clamped moderately thick cross-ply rectangular plates by superposition of exact untruncated infinite series solutions. J Reinforce Plast Compos 2005;24(16):1723–36.
[21] Umasree P, Bhaskar K. Analytical solutions for flexure of clamped rectangular cross-ply plates using an accurate zigzag type higher-order theory. Compos Struct 2006;74(4):426–39.
[22] Thornton DR, Conway HD. The structural analysis of edge-loaded plates. Int J Mech Sci 1980;22(8):481–90.